



Discover Generics

Cost-Effective CT & MRI Contrast Agents



WATCH VIDEO

AJNR

This information is current as of June 22, 2025.

The Predictive Value of 3D Time-of-Flight MR Angiography in Assessment of Brain Arteriovenous Malformation Obliteration after Radiosurgery

D.R. Buis, J.C.J. Bot, F. Barkhof, D.L. Knol, F.J. Lagerwaard, B.J. Slotman, W.P. Vandertop and R. van den Berg

AJNR Am J Neuroradiol 2012, 33 (2) 232-238

doi: <https://doi.org/10.3174/ajnr.A2744>

<http://www.ajnr.org/content/33/2/232>

ORIGINAL
RESEARCH

D.R. Buis
J.C.J. Bot
F. Barkhof
D.L. Knol
F.J. Lagerwaard
B.J. Slotman
W.P. Vandertop
R. van den Berg



The Predictive Value of 3D Time-of-Flight MR Angiography in Assessment of Brain Arteriovenous Malformation Obliteration after Radiosurgery

BACKGROUND AND PURPOSE: The purpose of radiosurgery of bAVMs is complete angiographic obliteration of its nidus. We assessed the diagnostic accuracy of 1.5T T2-weighted MR imaging and TOF-MRA images for detecting nidus obliteration after radiosurgery.

MATERIALS AND METHODS: The pre- and postradiosurgery MR images and DSA images from 120 patients who were radiosurgically treated for a bAVM were re-evaluated by 2 observers for patency of the nidus (preradiosurgery) and obliteration (postradiosurgery: final follow-up MR imaging), by using a 3-point scale of confidence. Consensus reading of the DSA after radiosurgery was considered the criterion standard for obliteration. Sensitivity, specificity, PPVs, and NPVs, and overall diagnostic performance by using ROC were determined.

RESULTS: Mean bAVM volume during radiosurgery was 3.4 mL (95% CI, 2.6–4.3 mL). Sixty-six patients (55%) had undergone previous endovascular embolization. The mean intervals between radiosurgery and follow-up MR imaging and for DSA, respectively, were 35.6 months (95% CI, 32.3–38.9 months) and 42.1 months (95% CI, 40.3–44.0 months). With ROC, an area under curve of 0.81–0.83 was found. PPVs and NPVs of final follow-up MR imaging for definitive obliteration varied between 0.85 and 0.95 and 0.55 and 0.62. An average false-positive rate, meaning overestimation of nidus obliteration, of 0.08 and an average false-negative rate, meaning underestimation of nidus obliteration of 0.48, were found.

CONCLUSIONS: MRA is insufficient to diagnose obliteration in the follow-up of bAVMs after radiosurgery. A remaining nidus diameter <10 mm seems to be the major limiting factor for reliable assessment of obliteration. We highly recommend follow-up DSA for definitive diagnosis of complete obliteration.

ABBREVIATIONS: bAVM = brain arteriovenous malformation; CI = confidence interval; 4D rCE-MRA = 4D radial-acquisition contrast-enhanced MRA; DO = definitive obliteration; DSA_{2C} = DSA uniform reference standard for obliteration; NPV = negative predictive value; PO = probable obliteration; PPV = positive predictive value; ROC = receiver operating characteristic analysis; TOF-MRA = time-of-flight MRA

Radiosurgery is an established technique for the treatment of bAVMs. Its purpose is to completely obliterate the nidus without causing new neurologic damage.¹ Its efficacy is high, and obliteration may be reached in 81% after 4 years and in 91% after 6 years.² The established method to evaluate nidus obliteration is DSA.

Although the neurologic risk of DSA is low with 0.09%–0.8% permanent neurologic deficits,^{3–8} silent embolisms were demonstrated after DSA on diffusion-weighted MR imaging in ≤23% of all cases.⁹ Other risks include bleeding, nephrotoxicity, and allergies.^{7,10,11} Moreover, patients regard DSA as an unpleasant examination due to its invasiveness, pain, and postprocedural bed rest.¹² Finally DSA carries inherent ioniz-

ing radiation risks, especially in children,^{13–15} and it is a costly investigation because it is labor-intensive and requires postprocedural hospitalization of the patient.¹⁶

High-contrast CTA has a proven ability to identify remnant bAVMs after radiosurgery,¹⁷ but similar to DSA, CTA carries risks of ionizing radiation and administration of contrast. Therefore, MR imaging evaluation may be a sensitive and noninvasive substitute.^{18–21} The risk of complications during an MR imaging examination of the brain is considerably lower, with no harmful effects reported in 1023 patients.²² In many institutions, MR imaging alone or in combination with MRA is used for radiologic follow-up; and in case of suspected obliteration or after a maximum follow-up time, patients are referred for DSA.^{23–27} We performed a retrospective analysis of 1.5T T2-weighted MR imaging and TOF-MRA to assess their ability to correctly predict nidus obliteration after radiosurgery, by using DSA as the criterion standard.

Materials and Methods

Between January 1998 and June 2007, 251 patients underwent radiosurgery for a bAVM at the VU University Medical Center. Our radiosurgical treatment protocol has been described before.²⁷ All patients were examined with MR imaging of the brain by using a 1.5T whole-

Received August 28, 2010; accepted after revision May 19, 2011.

From the Departments of Neurosurgery (D.R.B., W.P.V.), Neuroradiology (J.C.J.B., F.B.), Epidemiology and Biostatistics (D.L.K.), and Radiation Oncology (F.J.L., B.J.S.), Neurosurgical Center Amsterdam, VU University Medical Center, Amsterdam, the Netherlands; and Department of Radiology (R.v.d.B.), Academic Medical Center, Amsterdam, The Netherlands.

Please address correspondence to D.R. Buis, MD, PhD, Neurosurgical Center Amsterdam, VU University Medical Center, ZH 2F005, PO Box 7057, 1007MB Amsterdam, The Netherlands; e-mail: dr.buis@vumc.nl

<http://dx.doi.org/10.3174/ajnr.A2744>

body scanner, with a standard polarized head coil (Magnetom Vision, Magnetom Sonata; Siemens, Erlangen, Germany). The imaging protocol included T2-weighted MR imaging with a section thickness of 3 mm (TR, 3000 ms; TE, 20 ms) and TOF-MRA images (TR, 39 ms; TE, 6.5 ms; flip-angle, 20°) with a section thickness of 1 mm and an in-plane resolution of 0.4 mm. At the time of the study, the software for dynamic sequences was not available; therefore, no contrast enhancement was used.

On the day of radiosurgery, a stereotactic base ring (Brainlab, Feldkirchen, Germany) was attached to the patient's head under local anesthesia followed by a stereotactic DSA with a frame rate of 2–6 per second⁻¹. CTA with 2-mm section-thickness reconstructions with the stereotactic frame in place was performed. The DSA images were coregistered with the CT images by using the stereotactic localizer box. Finally, the MR imaging studies were digitally fused with the CT study by using the automatic image-fusion software of the radiosurgery planning system (BrainScan, Version 5.11 Brainlab). Follow-up included biennial MR imaging of the brain by using the above-mentioned sequences. MR imaging could be moved forward on clinical grounds. DSA was performed when MR imaging suggested complete obliteration. Alternatively, when no complete obliteration was observed on MR imaging at 4 years after radiosurgery, DSA was performed to assess the need for salvage treatment. Angiographic obliteration of the bAVM was defined as the complete absence of abnormal vessels in the former nidus of the malformation, with disappearance or normalization of early draining veins from the area and a normal circulation time on angiography.^{28,29}

Patient Selection

Included in this study were patients who were radiosurgically treated for a bAVM, in whom the bAVM was reported visible in the radiologic reports of MR imaging and DSA images obtained shortly before radiosurgery (MR imaging₁ and DSA₁), and in whom final follow-up MR imaging and DSA studies (MR imaging₂ and DSA₂) were performed. bAVMs that were not visible on MR imaging₁ were excluded from further analysis. From a cohort of 251 patients, these criteria led to the inclusion of 120 patients. All imaging series were independently reviewed by 2 experienced neuroradiologists on the local PACS system. DSA₁ images were reviewed for visibility of the nidus, size, drainage pattern, and eloquence of the bAVM. From these data, the Spetzler-Martin gradation was derived.³⁰ Follow-up MR images were examined for patency of the bAVM. bAVM obliteration on MR imaging was assessed by using a 3-point scale: patent, PO, and DO. DSA₂ images were reviewed for the presence of partial or complete obliteration. In case of partial obliteration, the maximum diameter of the remaining nidus was measured.

Each series of examinations was reviewed for each patient in a strict sequence simulating normal clinical practice: MR imaging₁, DSA₁; MR imaging₂, DSA₂. To simulate the actual clinical situation, we did not blind our observers to the patient's clinical situation, in contrast to some comparable studies.^{19,31–34} All DSA₂ images were re-evaluated for the presence of obliteration in a consensus meeting to create a uniform reference standard (DSA_{2c}).

Clinical and treatment parameters noted included sex, clinical presentation, age at time of radiosurgery, marginal dose, volume and location of the bAVM, previous partial or unsuccessful treatment, and length of follow-up. The modified bAVM-score of Pollock and Flickinger³⁵ was derived from these data.

Table 1: Presentation and location of 120 bAVMs

Location	No. (%)	Presentation	No. (%)
Frontal	25 (20.8)	Seizures	40 (33.3)
Temporal	30 (25.0)	Parenchymal hemorrhage	40 (33.3)
Parietal	22 (18.3)	Subarachnoid hemorrhage	5 (4.2)
Occipital	14 (11.7)	Intraventricular hemorrhage	8 (6.7)
Basal ganglia	1 (0.8)	Focal neurologic deficit	4 (3.3)
Thalamic	13 (10.8)	Headache	13 (10.8)
Cerebellum	9 (7.5)	Screening	10 (8.3)
Brain stem	1 (0.8)		
Periventricular	1 (0.8)		
Corpus callosum	4 (3.3)		

Statistics

Sensitivity, specificity, NPV, and PPV for obliteration were determined. "Sensitivity" was defined as the probability of finding obliteration on MR imaging₂ among those images demonstrating complete obliteration on DSA_{2c}. "Specificity" was defined as the probability of finding a patent nidus among those whose images demonstrated no obliteration on DSA_{2c}. "NPV" was defined as the percentage of patients among whom the nidus was diagnosed as patent on MR imaging₂ and in whom this was confirmed on DSA_{2c}. "PPV" was defined as the percentage of patients among whom the nidus was diagnosed as obliterated on MR imaging₂ and in whom this was confirmed on DSA_{2c}.

For differentiating a patent from an obliterated bAVM on MR imaging₂ in comparison with DSA_{2c}, ROC analysis per observer was performed.³⁶

A univariate regression analysis was performed to assess which factors (Spetzler-Martin grade, drainage pattern, previous embolization, and interval between MR imaging₂ and DSA₂) correlated with discrepant findings between MR imaging₂ and DSA_{2c}. All statistics were performed by using the Statistical Package for the Social Sciences, Version 17.0 (SPSS, Chicago, Illinois).

Results

One hundred twenty series of images from 120 patients were included in this study (Table 1). There were 56 females and 64 males. Lateralization was right ($n = 44$), midline ($n = 5$), or left ($n = 71$). Mean bAVM volume during radiosurgery was 3.4 mL (95% CI, 2.6–4.3 mL), with a mean marginal dose administered to the 80% isodose line of 1917 cGy (95% CI, 1878–1956 cGy). Mean age at radiosurgery was 37.5 years (95% CI, 35.9–39.0 years). Sixty-six patients (55%) had undergone previous endovascular embolization. Spetzler-Martin grades were 1 ($n = 20$), 2 ($n = 39$), 3 ($n = 48$), or 4 ($n = 13$). The mean modified bAVM score was 1.15 (95% CI, 1.1–1.2).

All DSA₁ investigations were made on the day of radiosurgery. The mean interval between MR imaging₁ and radiosurgery was −4.5 days (range, −211–7 days; median, −1 day). The mean intervals between radiosurgery and MR imaging₂ and radiosurgery and DSA₂, respectively, were 35.6 months (95% CI, 32.3–38.9 months) and 42.1 months (95% CI, 40.3–44.0 months). The interval between MR imaging₂ and DSA₂ was ≤3 months ($n = 48$, 40%), between 3 and 6 months ($n = 39$, 32.5%), or >6 months ($n = 33$, 27.5%). No DSA- or MR imaging-related complications occurred.

Each series of images ($n = 120$) was reviewed by both observers (240 patient series). Both observers could not deter-

Table 2: bAVM qualities, as determined on DSA ₁			
bAVM	Qualities	Observer 1 (n = 117)	Observer 2 (n = 117)
Size	Small,	85	83
	medium,	32	33
	large	0	1
Drainage	Superficial,	70	62
	deep,	47	53
	N/A ^a		2
Eloquence	Eloquent,	25	55
	not eloquent	92	62

Note:—N/A indicates not applicable.

^aObserver 2 could not determine the drainage pattern in 2 patients.

Table 3: Determination of nidus obliteration on MRI ₂						
DSA _{2c}	MRI ₂ Observer 1 (n = 117)			MRI ₂ Observer 2 (n = 117)		
	Patent	PO	DO	Patent	PO	DO
Patent	32	1	6	36	2	2
Obliterated	15	15	48	21	14	42
	47	16	54	57	16	44

Table 4: Predictive value of MRI ₂ for definitive obliteration in comparison with DSA _{2c}		
	Observer 1	Observer 2
Sensitivity	0.52	0.52
Specificity	0.89	0.95
PPV	0.85	0.95
NPV	0.62	0.55
Prevalence	0.54	0.62
False-positive rate	0.10	0.04
False-negative rate	0.48	0.48

mine nidus patency in 2 separate patients each and agreed on nondetermination of nidus patency in 1 more patient. Therefore, 6 patient series based on 5 patients were discarded from further analysis. Statistical analysis was based on the reviews of DSA₁, MR imaging₂, and DSA₂ in 234 patient series (117 patients each, Table 2).

Definitive obliteration was determined on MR imaging₂ by observers 1 and 2 in 46% and 38%, respectively (Table 3).

PPV and NPV of MR imaging₂ for definitive obliteration varied between 0.85 and 0.95 and 0.55 and 0.62 (Table 4).

Among the 98 observations of definitive obliteration on MR imaging₂, 8 observations in 6 patients still demonstrated a patent nidus on DSA_{2c} for a false-positive rate of 0.08 (Fig 1A). In 7 of these 8 observations, the remaining nidus was estimated to be <10 mm (Table 5). In the other 90 observations, complete obliteration was confirmed angiographically (Fig 1B).

Conversely, among the 136 observations of partial obliteration or a patent nidus on MR imaging₂, 65 demonstrated complete obliteration on DSA_{2c} for a false-negative rate of 0.48 (Fig 1C). In the other 71 observations, the presence of a remnant nidus was confirmed angiographically (Fig 1D).

Among the patients who failed to demonstrate complete obliteration on DSA_{2c}, the mean size of the remaining nidus, as measured on DSA₂ was 12 mm (9–16 mm), as assessed by observer 1 (n = 39) and 15 mm (10–20 mm) as assessed by observer 2 (n = 40).

For differentiating a patent from an obliterated bAVM on

MR imaging₂ in comparison with DSA_{2c}, ROC demonstrated an area under the ROC curve for predicting obliteration varying between 0.81 and 0.83 (Fig 2).

In a univariate regression analysis, bAVM volume, Spetzler-Martin grade, drainage pattern, previous embolization, and interval between MR imaging₂ and DSA₂ were not found to be significant factors for determination of obliteration on MR imaging₂.

Discussion

Previous studies showed a decrease of 54% in overall risk of hemorrhage after radiosurgery before obliteration and a further decrease of 88% after obliteration.² Moreover, others proposed that especially small niduses bleed.³⁷ Therefore, the end point in radiosurgery of bAVMs should be complete obliteration of the nidus. Due to its high spatial and temporal resolution, DSA is the reference technique for judging obliteration.^{28,29,38} Although the clinical risks of being subjected to DSA remain low,^{3–8} this risk increases when multiple consecutive cerebral angiographies are performed, such as in patients with bAVMs. MR imaging has practically no risk.²² In a previous study, we demonstrated that MRA-based images might be used as the sole imaging technique for radiosurgery of bAVMs <3 mL when in a noneloquent location.³⁹

In this study, we aimed to answer the question of whether MRA can be used to predict obliteration reliably and, therefore, whether MRA can replace DSA in the follow-up of bAVMs after radiosurgery. We found an average false-positive rate of 0.08 for 2 observers, which is comparable with that in other studies.^{40,41} A false-negative rate of 0.48 was found.

These findings may have serious consequences. Because partial nidus obliteration does not offer protection,² overestimation of the true obliteration rate may result in insufficient additional therapy or on an increased population of patients with an intracranial hemorrhage after complete obliteration was falsely diagnosed. On the basis of our data, a small remaining nidus, <10 mm diameter, seems to be the major cause for overestimation of nidus obliteration. Mukherji et al⁴² demonstrated similar findings with at least 95% sensitivity and 100% specificity for depicting a residual nidus, provided that an arteriovenous shunt and a residual nidus of >1 cm remain. With gradient-echo imaging, the sensitivity did not become <100% until the nidus diameter was <0.36 cm.

Without contrast, 1.5T MRA could detect 81%–100% of intracranial vessels with a diameter ≤1 mm in comparison with DSA.⁴³ Because MRA measures blood flow, we postulate that the progressive endothelial proliferation, during the process of (partial) obliteration,⁴⁴ leads to a reduction in both vessel numbers and diameters, which subsequently diminishes the blood flow below the perceptibility threshold of 1.5T MRA. Because more and smaller cerebral vessels can be found by using a higher field strength,⁴⁵ this solution may be applicable in diagnosing remaining niduses, because they are in the process of gradual obliteration. Recently, more sophisticated MR imaging techniques were developed that have demonstrated improved depiction of bAVMs in small series, but cutoff points for diagnosing obliteration were not given.^{18,21,31–33,46}

In a study of nidus delineation on MRA in comparison with DSA, bAVMs delineated on MRA were found to be larger and more randomly displaced.³⁹ We studied bAVMs after radio-

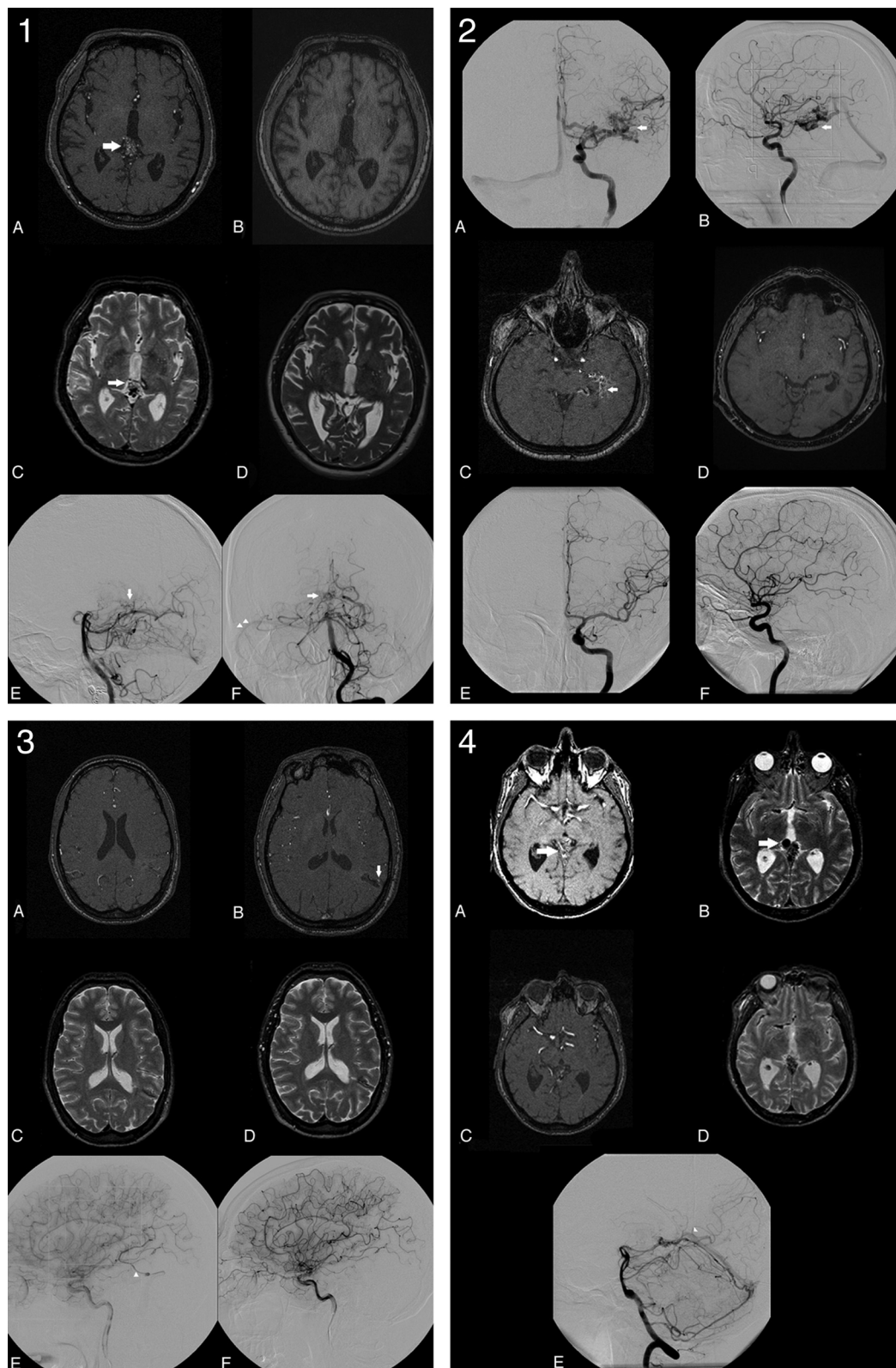


Fig 1. 1, Overestimation of nidus obliteration: a 0.90-mL tectal bAVM, which is clearly visible on MR imaging₁ (A and C white arrows). A–F, Both observers determined this bAVM to be obliterated on MR imaging₂ (B and D) almost 3 years later. However DSA₂, performed 6 weeks after MR imaging₂, still demonstrates a small nidus (E and F, white arrows) with early venous drainage toward the lateral sinus (F, white arrowheads). 2, Successful determination of nidus obliteration in the case of a 3.68-mL-deep temporal bAVM (straight white arrow, A–C). On the basis of MR imaging₂, both observers agreed that the nidus was obliterated 25 months after radiosurgery (D). Obliteration was angiographically confirmed 6 weeks later (E and F). 3, Underestimation of nidus obliteration: a small 0.17-mL central bAVM that was previously partially treated by endovascular embolization (A, C, and E). Because of hyperintensity on MR imaging₂ (B, white vertical arrow), both observers judged this bAVM to be patent 1 year after radiosurgery (B and D). However DSA₂ (F), performed 2 months after MR imaging₂, demonstrates absence of the previously present early venous drainage (E, white arrowhead). 4, Successful determination of a remaining nidus in case of a patent 2.32-mL tectal bAVM (white horizontal arrow, A and B). On the basis of MR imaging₂, both observers agreed that the nidus was patent 4 years after radiosurgery (C and D). The presence of a remnant nidus was angiographically confirmed 6 weeks later, when early venous drainage toward the straight sinus was observed (white arrowhead, E).

Table 5: Over- and underestimation of nidus obliteration on MRI₂

	Overestimation of Nidus Obliteration on MRI ₂ (n = 6 patients, 8 observations)	Underestimation of Nidus Obliteration on MRI ₂ (n = 49 patients, 65 observations)
Mean age (yr)	29.3 (14.0–44.7) ^a	37.4 (33.1–41.7) ^a
bAVM volume (mL)	4.3 (0.2–8.5) ^a	3.3 (2.3–4.2) ^a
bAVM score	1.10 (0.57–1.63) ^a	1.11 (0.98–1.25) ^a
SM gradation (%)		
I	1 (17%)	9 (18.4%)
II	0	21 (42.9%)
III	4 (67%)	16 (32.7%)
IV	1 (17%)	2 (4.1%)
V	0	0
Unclassifiable	N/A	1 (2.0%)
Drainage (%)		
Superficial	2 (33%)	32 (65.3%)
Deep	4 (67%)	16 (32.7%)
Unclassifiable	N/A	1 (2.0%)
Previous embolization (%)	2 (33%)	30 (61.2%)
Treatment dose (cGy)	1900 (1643–2157) ^a	1935 (1874–1996) ^a
Location (%)		
Corpus callosum	N/A	1 (2%)
Cerebellum	N/A	6 (12.2%)
Frontal	N/A	11 (22.4%)
Occipital	2 (33%)	7 (14.3%)
Parietal	2 (33%)	11 (22.4%)
Temporal	1 (17%)	10 (20.4%)
Thalamic	1 (17%)	3 (6.1%)
Interval MRI ₂ -DSA ₂ (mo)	7.1 (4.1–10.1) ^a	2.5 (0.5–4.6) ^a

Note:—N/A, not applicable, SM, Spetzler-Martin grade.

^aThe ranges in parentheses refer to the 95% CI.

surgery and found the opposite. Furthermore, it is of interest to mention that among 14 patients in whom complete obliteration was diagnosed by using MRA, Giesel et al¹⁷, using high contrast CTA, were able to demonstrate a residual nidus in 2 and subtotal obliteration in 3 more patients, suggesting that CTA may be an alternative for detecting residual nidus.

Conversely, misdiagnosing an obliterated nidus for a patient one means that the patient has the disease for a longer interval and may be subjected to additional and unnecessary therapy. The cause for the poor NPV might be the absence of a regular T1 sequence in our follow-up protocol. T1 sequences have very short TRs, which result in saturation of all static tissues, except for tissues with a very short T1 relaxation time, such as hematoma or coagulated blood. Because 3D TOF-MRA is also a T1-based technique, coagulated or slow-flowing blood might present as hyperintense signal intensity as well. The combination of T1 and 3D TOF-MRA might overcome misinterpreting stagnation of nidus blood flow as persistent flow. The drawback of our follow-up protocol is the inability to make this differentiation. This may have resulted in underestimation of nidus obliteration because some 3D TOF-MRA sequences may demonstrate hyperintensity due to the presence of coagulated blood.

Other factors that may have affected the performance of MR imaging could be the relatively long time interval (>6 months in 28% of the population) between MR imaging₂ and DSA₂. This interval may lead to overestimation of obliteration on MR imaging when the interval is short and the nidus approaches obliteration with a slow intranidal blood flow. Conversely, this interval may lead to underestimation of obliteration on MRA when a clearly visible nidus obliterates completely during a long interval between MR imaging₂ and

DSA₂. Nevertheless, in the present study a univariate regression analysis demonstrated that this factor did not contribute significantly to determining obliteration on MR imaging₂.

The major limitation by using non-contrast-enhanced 1.5T T2-weighted MR imaging and TOF-MRA images to determine nidus obliteration is a lack of temporal resolution. This might explain a worse outcome in comparison with other studies that report a sensitivity varying between 80% and 100% for detection of residual nidus.^{40,41,47} With these dynamic contrast-enhanced MRA sequences, the temporal resolution is 1 frame per 1.7 seconds, in comparison with 6 images per second for DSA. However, the signal intensity-to-noise ratio for such dynamic contrast-enhanced MRA sequences is better than that of 3D TOF-MRA. In addition 3D TOF-MRA is known to have spin dephasing due to complex or turbulent flow patterns, as well as signal-intensity saturation in areas of slow flow.⁴⁸ Due to these shortcomings, isolating venous drainage, depicting slow flow or a small nidus, becomes more difficult.⁴¹ These shortcomings become exaggerated in the absence of gadolinium because gadolinium confers a high sensitivity to slow flow due to its T1 shortening effect, with rare saturation effects.⁴⁹

Recently other studies, using far more sophisticated MR imaging sequences, have been published.^{19–21,31,33,34,46,50} Currently, the most promising technique for depicting a residual nidus may be 4D rCE-MRA, in which a combination of several MR imaging techniques, such as radial undersampling, sliding window reconstruction, and sliding mask subtraction, are used, which leads to a sufficiently high temporal and spatial resolution, so that all phases of the intracranial circulation can be separated adequately. Using this MR imaging technique in comparison with DSA, 3 ob-

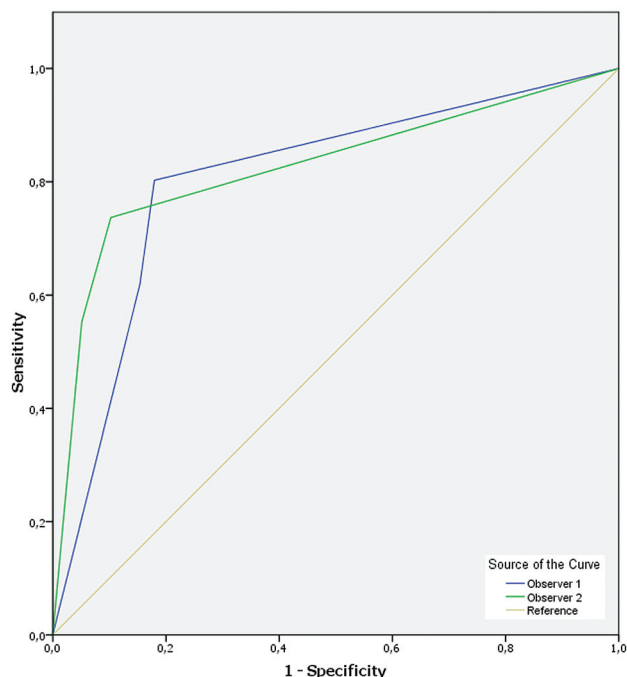


Fig 2. ROC demonstrates an area under the ROC curve for predicting obliteration of 0.81–0.83 for each individual observer.

servers were able to correctly identify nidus size and location, arterial feeders, and drainage pattern in 13 patients with bAVMs. The Spetzler-Martin grade was correctly assessed in all except 1.¹⁸ However, the spatial resolution of 4D rCE-MRA is on the order of 1 mm¹⁸; therefore, even this sophisticated technique may miss a small remnant nidus.

Conclusions

In our institution, we use consecutive MR imaging investigations to determine whether nidus obliteration has occurred. Our findings are somewhat disappointing. Although MRA may be used to follow the process of progressive obliteration, as long as the nidus remains clearly visible, it is an insufficient investigation for diagnosing obliteration in the follow-up of bAVMs after radiosurgery. A remaining nidus diameter of <10 mm seems to be the major limiting factor for reliable assessment of obliteration. Other authors found that bAVMs that are misdiagnosed as obliterated on MR imaging are likely to be either small or drain into a single vein.^{40,51} Although such a configuration was found in conjunction with an increased obliteration rate or even spontaneous obliteration,^{52,53} the clinical course of a partially obliterated nidus remains unpredictable, with 23 reported hemorrhages before obliteration among 458 patients who were radiosurgically treated for a bAVM.² The importance of performing DSA to rule out a persistent nidus after radiosurgery has been stressed before.⁵⁴ Because reasons for still performing DSA include the limited diagnostic performance of 3D-TOF-MRA, a lower morbidity rate during cerebral angiographic procedures in young patients,^{3,5,8} and the above-mentioned consequences of misdiagnosing a patent nidus, we agree with this point of view. Because the potential consequences of bleeding from a bAVM and potential morbidity due to cerebral angiography are known but the odds of bleeding due to a persistent nidus re-

main unknown, and taking into account that newer MR imaging modalities demonstrate an improved depiction of the nidus, a large prospective study in which follow-up by using dynamic contrast-enhanced MRA and DSA versus dynamic contrast-enhanced MRA imaging only are compared, might be appropriate.

Meanwhile MRA is an excellent and low-invasive imaging technique to follow the process of progressive obliteration. On the basis of our findings, we did not change our follow-up protocol, though presently we are using contrast-enhanced MRA. We recommend performing MR imaging every 2 years after radiosurgery to demonstrate obliteration of the nidus. On the basis of the aforementioned data, obliteration, as shown on MRA, should be confirmed on DSA. When obliteration fails to occur, DSA should be performed to assess the possibilities for treatment, which may include repeat radiosurgery.⁵⁵ When obliteration fails to occur after repeat radiosurgery, a wait-and-see policy should be initiated, unless the smaller bAVM can clearly be obliterated by means of endovascular embolization.

Disclosures: Frederik Barkhof, *Research Support* (including provision of equipment or materials): Siemens, GE Healthcare, Details: Both provided software and pulse-sequence for research collaborations; *Consultant*: GE Healthcare, Details: Neuro-MRI advisory board. Ben Slotman, *Research Support* (including provision of equipment or materials): Varian Medical Systems, Brainlab, Details: master research agreement with both companies; *Speaker Bureau*: Varian Medical Systems, Brainlab, Details: speaker for both companies. *Consultant*: Varian Medical Systems.

References

1. Friedlander RM. **Clinical practice: arteriovenous malformations of the brain.** *N Engl J Med* 2007;356:2704–12
2. Maruyama K, Kawahara N, Shin M, et al. **The risk of hemorrhage after radiosurgery for cerebral arteriovenous malformations.** *N Engl J Med* 2005;352:146–53
3. Heiserman JE, Dean BL, Hodak JA, et al. **Neurologic complications of cerebral angiography.** *AJNR Am J Neuroradiol* 1994;15:1401–07
4. Dion JE, Gates PC, Fox AJ, et al. **Clinical events following neuroangiography: a prospective study.** *Stroke* 1987;18:997–1004
5. Earnest F, Forbes G, Sandok BA, et al. **Complications of cerebral angiography: prospective assessment of risk.** *AJR Am J Roentgenol* 1984;142:247–53
6. Komiyama M, Yamanaka K, Nishikawa M, et al. **Prospective analysis of complications of catheter cerebral angiography in the digital subtraction angiography and magnetic resonance era.** *Neurol Med Chir (Tokyo)* 1998;38:534–39
7. Dawkins AA, Evans AL, Wattam J, et al. **Complications of cerebral angiography: a prospective analysis of 2,924 consecutive procedures.** *Neuroradiology* 2007;49:753–59
8. Grzyska U, Freitag J, Zeumer H. **Selective cerebral intraarterial DSA. Complication rate and control of risk factors.** *Neuroradiology* 1990;32:296–99
9. Bendszus M, Koltzenburg M, Burger R, et al. **Silent embolism in diagnostic cerebral angiography and neurointerventional procedures: a prospective study.** *Lancet* 1999;354:1594–97
10. Morcos SK, Thomsen HS. **Adverse reactions to iodinated contrast media.** *Eur Radiol* 2001;11:1267–75
11. Ketkar M, Shrier D. **An allergic reaction to intraarterial nonionic contrast material.** *AJNR Am J Neuroradiol* 2003;24:292
12. King-Im JM, Trivedi R, Cross J, et al. **Conventional digital subtraction x-ray angiography versus magnetic resonance angiography in the evaluation of carotid disease: patient satisfaction and preferences.** *Clin Radiol* 2004;59:358–63
13. Thierry-Chef I, Simon S, Miller D. **Radiation dose and cancer risk among pediatric patients undergoing interventional neuroradiology procedures.** *Pediatr Radiol* 2006;36:159–62
14. Swoboda NA, Armstrong DG, Smith J, et al. **Pediatric patient surface doses in neuroangiography.** *Pediatr Radiol* 2005;35:859–66
15. Raelson CA, Kanal KM, Vavilala MS, et al. **Radiation dose and excess risk of cancer in children undergoing neuroangiography.** *Am J Roentgenol* 2009;193:1621–28
16. Stein SC, Burnett MG, Zager EL, et al. **Completion angiography for surgically treated cerebral aneurysms: an economic analysis.** *Neurosurgery* 2007;61:1162–67
17. Giesel FL, Essig M, Zabel-Du-Bois A, et al. **High-contrast computed tomographic angiography better detects residual intracranial arteriovenous mal-**

- formations in long-term follow-up after radiotherapy than 1.5-Tesla time-of-flight magnetic resonance angiography. *Acta Radiol* 2010;51:64–70
18. Eddleman CS, Jeong HJ, Hurley MC, et al. 4D radial acquisition contrast-enhanced MR angiography and intracranial arteriovenous malformations: quickly approaching digital subtraction angiography. *Stroke* 2009;40:2749–53
 19. Hadizadeh DR, von Falkenhausen M, Gieseke J, et al. Cerebral arteriovenous malformation: Spetzler-Martin classification at subsecond-temporal-resolution four-dimensional MR angiography compared with that at DSA. *Radiology* 2008;246:205–13. Epub 2007 Oct 19
 20. Reinacher PC, Stracke P, Reinges MH, et al. Contrast-enhanced time-resolved 3-D MRA: applications in neurosurgery and interventional neuroradiology. *Neuroradiology* 2007;49(suppl 1):S3–13
 21. Taschner CA, Gieseke J, Le Thuc V, et al. Intracranial arteriovenous malformation: time-resolved contrast-enhanced MR angiography with combination of parallel imaging, keyhole acquisition, and k-space sampling techniques at 1.5 T. *Radiology* 2008;246:871–79. Epub 2008 Jan 14
 22. Weintraub MI, Khoury A, Cole SP. Biologic effects of 3 Tesla (T) MR imaging comparing traditional 1.5 T and 0.6 T in 1023 consecutive outpatients. *J Neuroimaging* 2007;17:241–45
 23. Han JH, Kim DG, Chung HT, et al. Clinical and neuroimaging outcome of cerebral arteriovenous malformations after gamma knife surgery: analysis of the radiation injury rate depending on the arteriovenous malformation volume. *J Neurosurg* 2008;109:191–98
 24. Douglas JG, Goodkin R. Treatment of arteriovenous malformations using gamma knife surgery: the experience at the University of Washington from 2000 to 2005. *J Neurosurg* 2008;109(suppl):51–56
 25. Kasliwal MK, Kale SS, Gupta A, et al. Outcome after hemorrhage following gamma knife surgery for cerebral arteriovenous malformations. *J Neurosurg* 2009;110:1003–09
 26. Kiran N, Kale S, Kasliwal M, et al. Gamma knife radiosurgery for arteriovenous malformations of basal ganglia, thalamus and brainstem: a retrospective study comparing the results with that for AVMs at other intracranial locations. *Acta Neurochir (Wien)* 2009;151:1575–82. Epub 2009 May 5
 27. Buis DR, Dirven CM, Lagerwaard FJ, et al. Radiosurgery of brain arteriovenous malformations in children. *J Neurol* 2008;255:551–60
 28. Lindquist C, Steiner L. Stereotactic radiosurgical treatment of arteriovenous malformations. In: Lunsford LD, ed. *Modern Stereotactic Neurosurgery*. Boston, Massachusetts: Martinus Nijhoff; 1988:491–505
 29. Steinberg GK, Fabrikant JI, Marks MP, et al. Stereotactic heavy-charged-particle Bragg-peak radiation for intracranial arteriovenous malformations. *N Engl J Med* 1990;323:96–101
 30. Spetzler RF, Martin NA. A proposed grading system for arteriovenous malformations. *J Neurosurg* 1986;65:476–83
 31. Petkova M, Gauvrit JY, Trystram D, et al. Three-dimensional dynamic time-resolved contrast-enhanced MRA using parallel imaging and a variable rate k-space sampling strategy in intracranial arteriovenous malformations. *J Magn Reson Imaging* 2009;29:7–12
 32. Kunishima K, Mori H, Itoh D, et al. Assessment of arteriovenous malformations with 3-Tesla time-resolved, contrast-enhanced, three-dimensional magnetic resonance angiography. *J Neurosurg* 2009;110:492–99
 33. Saleh RS, Lohan DG, Villablanca JP, et al. Assessment of craniospinal arteriovenous malformations at 3T with highly temporally and highly spatially resolved contrast-enhanced MR angiography. *AJNR Am J Neuroradiol* 2008;29:1024–31
 34. Heidenreich JO, Schilling AM, Unterharnscheidt F, et al. Assessment of 3D-TOF-MRA at 3.0 Tesla in the characterization of the angioarchitecture of cerebral arteriovenous malformations: a preliminary study. *Acta Radiol* 2007;48:678–86
 35. Pollock BE, Flickinger JC. Modification of the radiosurgery-based arteriovenous malformation grading system. *Neurosurgery* 2008;63:239–43
 36. Metz C. ROC analysis in medical imaging: a tutorial review of the literature. *Radiol Phys Technol* 2008;1:2–12
 37. Spetzler RF, Hargraves RW, McCormick PW, et al. Relationship of perfusion pressure and size to risk of hemorrhage from arteriovenous malformations. *J Neurosurg* 1992;76:918–23
 38. Oppenheim C, Meder JF, Trystram D, et al. Radiosurgery of cerebral arteriovenous malformations: is an early angiogram needed? *AJNR Am J Neuroradiol* 1999;20:475–81
 39. Buis DR, Lagerwaard FJ, Dirven CM, et al. Delineation of brain AVMs on MR-angiography for the purpose of stereotactic radiosurgery. *Int J Radiat Oncol Biol Phys* 2007;67:308–16
 40. Pollock BE, Kondziolka D, Flickinger JC, et al. Magnetic resonance imaging: an accurate method to evaluate arteriovenous malformations after stereotactic radiosurgery. *J Neurosurg* 1996;85:1044–49
 41. Gauvrit JY, Oppenheim C, Nataf F, et al. Three-dimensional dynamic magnetic resonance angiography for the evaluation of radiosurgically treated cerebral arteriovenous malformations. *Eur Radiol* 2006;16:583–91
 42. Mukherji SK, Quisling RG, Kubilis PS, et al. Intracranial arteriovenous malformations: quantitative analysis of magnitude contrast MR angiography versus gradient-echo MR imaging versus conventional angiography. *Radiology* 1995;196:187–93
 43. Stock KW, Wetzel S, Kirsch E, et al. Anatomic evaluation of the circle of Willis: MR angiography versus intraarterial digital subtraction angiography. *AJNR Am J Neuroradiol* 1996;17:1495–99
 44. Buis DR, van den Berg R, Lagerwaard FJ, et al. Brain arteriovenous malformations: from diagnosis to treatment. *J Neurosurg Sci* 2011;55:39–56
 45. Nowinski WL, Puspitasari F, Volkau I, et al. Comparison of magnetic resonance angiography scans on 1.5, 3, and 7 Tesla units: a quantitative study of 3-dimensional cerebrovasculature. *J Neuroimaging* 2011 Mar 29. [Epub ahead of print]
 46. Saleh RS, Singhal A, Lohan D, et al. Assessment of cerebral arteriovenous malformations with high temporal and spatial resolution contrast-enhanced magnetic resonance angiography: a review from protocol to clinical application. *Top Magn Reson Imaging* 2008;19:251–57
 47. Lee KE, Choi CG, Choi JW, et al. Detection of residual brain arteriovenous malformations after radiosurgery: diagnostic accuracy of contrast-enhanced three-dimensional time of flight MR angiography at 3.0 Tesla. *Korean J Radiol* 2009;10:333–39
 48. Ozsarlak O, Van Goethem JW, Maes M, et al. MR angiography of the intracranial vessels: technical aspects and clinical applications. *Neuroradiology* 2004;46:955–72
 49. Unlu E, Temizoz O, Albayram S, et al. Contrast-enhanced MR 3D angiography in the assessment of brain AVMs. *Eur J Radiol* 2006;60:367–78
 50. Parmar H, Ivancevic MK, Dudek N, et al. Neuroradiologic applications of dynamic MR angiography at 3 T. *Magn Reson Imaging Clin N Am* 2009;17:63–75
 51. Yen CP, Varady P, Sheehan J, et al. Subtotal obliteration of cerebral arteriovenous malformations after gamma knife surgery. *J Neurosurg* 2007;106:361–69
 52. Buis DR, van den Berg R, Lycklama G, et al. Spontaneous regression of brain arteriovenous malformations: a clinical study and a systematic review of the literature. *J Neurol* 2004;251:1375–82
 53. van den Berg R, Buis DR, Lagerwaard FJ, et al. Extensive white matter changes after stereotactic radiosurgery for brain arteriovenous malformations: a prognostic sign for obliteration? *Neurosurgery* 2008;63:1064–69
 54. Schaller C, Schramm J. Arteriovenous malformations and magnetic resonance imaging. *J Neurosurg* 1997;87:647–49
 55. Buis DR, Meijer OW, van den Berg R, et al. Clinical outcome after repeated radiosurgery for brain arteriovenous malformations. *Radiother Oncol* 2010;95:250–56